



Differing Patterns of Selection and Geospatial Genetic Diversity within Two Leading *Plasmodium vivax* Candidate Vaccine Antigens

Christian M. Parobek^{1,2*}, Jeffrey A. Bailey^{3,4}, Nicholas J. Hathaway^{3,5}, Duong Socheat⁶, William O. Rogers⁷, Jonathan J. Juliano⁸

1 School of Medicine, University of North Carolina, Chapel Hill, North Carolina, United States of America, **2** Curriculum in Genetics and Molecular Biology, University of North Carolina, Chapel Hill, North Carolina, United States of America, **3** Program in Bioinformatics and Integrative Biology, University of Massachusetts, Worcester, Massachusetts, United States of America, **4** Division of Transfusion Medicine, School of Medicine, University of Massachusetts Medical School, Worcester, Massachusetts, United States of America, **5** School of Medicine, University of Massachusetts, Worcester, Massachusetts, United States of America, **6** National Malaria Center, Phnom Penh, Cambodia, **7** United States Navy, Naval Medical Research Unit #2, Phnom Penh, Cambodia, **8** Division of Infectious Diseases, University of North Carolina School of Medicine, Chapel Hill, North Carolina, United States of America

Abstract

Although *Plasmodium vivax* is a leading cause of malaria around the world, only a handful of vivax antigens are being studied for vaccine development. Here, we investigated genetic signatures of selection and geospatial genetic diversity of two leading vivax vaccine antigens – *Plasmodium vivax* merozoite surface protein 1 (*pvmsp-1*) and *Plasmodium vivax* circumsporozoite protein (*pvcsp*). Using scalable next-generation sequencing, we deep-sequenced amplicons of the 42 kDa region of *pvmsp-1* (n=44) and the complete gene of *pvcsp* (n=47) from Cambodian isolates. These sequences were then compared with global parasite populations obtained from GenBank. Using a combination of statistical and phylogenetic methods to assess for selection and population structure, we found strong evidence of balancing selection in the 42 kDa region of *pvmsp-1*, which varied significantly over the length of the gene, consistent with immune-mediated selection. In *pvcsp*, the highly variable central repeat region also showed patterns consistent with immune selection, which were lacking outside the repeat. The patterns of selection seen in both genes differed from their *P. falciparum* orthologs. In addition, we found that, similar to merozoite antigens from *P. falciparum* malaria, genetic diversity of *pvmsp-1* sequences showed no geographic clustering, while the non-merozoite antigen, *pvcsp*, showed strong geographic clustering. These findings suggest that while immune selection may act on both vivax vaccine candidate antigens, the geographic distribution of genetic variability differs greatly between these two genes. The selective forces driving this diversification could lead to antigen escape and vaccine failure. Better understanding the geographic distribution of genetic variability in vaccine candidate antigens will be key to designing and implementing efficacious vaccines.

Citation: Parobek CM, Bailey JA, Hathaway NJ, Socheat D, Rogers WO, et al. (2014) Differing Patterns of Selection and Geospatial Genetic Diversity within Two Leading *Plasmodium vivax* Candidate Vaccine Antigens. PLoS Negl Trop Dis 8(4): e2796. doi:10.1371/journal.pntd.0002796

Editor: Mauricio Martins Rodrigues, Federal University of São Paulo, Brazil

Received: August 12, 2013; **Accepted:** March 5, 2014; **Published:** April 17, 2014

This is an open-access article, free of all copyright, and may be freely reproduced, distributed, transmitted, modified, built upon, or otherwise used by anyone for any lawful purpose. The work is made available under the Creative Commons CC0 public domain dedication.

Funding: This work was supported by the US Department of Defense Global Emerging Infections Surveillance and Response System (DoD-GEIS) Program (for funding of the clinical trial), the University of North Carolina Research Council (UL1TR000083) and from the National Institutes of Health (AI089819 to JJJ). CMP was supported by the UNC MD/PhD Program (T32 GM008719) and Genetics Curriculum (T32 GM007092) and a grant from the Infectious Disease Society of America Medical Scholars Program. The views expressed in this paper are those of the authors and do not represent the official position of the U.S. Department of Defense, NIH, or UNC Chapel Hill. The funders had no role in study design, data collection and analysis, decision to publish, or preparation of the manuscript.

Competing Interests: The authors have declared that no competing interests exist.

* E-mail: christian_parobek@med.unc.edu

Introduction

Plasmodium vivax causes 80 to 300 million infections per year and over 2.5 billion people remain at risk of infection despite malaria elimination efforts [1]. Now, concern over *P. vivax* is growing due to reports of increasingly severe disease [2], emerging chloroquine resistance [3], and multi-drug resistance [4]. Ultimately, an effective vaccine will be important for controlling *P. vivax* malaria [5]. The fact that humans naturally develop partial immunity to *P. vivax* and *P. falciparum* lends hope for effective vaccines against these parasites; however, because the majority of global malaria research funding targets *P. falciparum* [6,7], only a handful of *P. vivax* antigens are currently being considered for vaccine development [8]. Among these are *P. vivax* merozoite surface protein 1 (*pvmsp-1*) and circumsporozoite protein (*pvcsp*).

PvMSP-1, an erythrocytic vaccine candidate, plays an important role in reticulocyte invasion [9]. Its C-terminus contains a 42 kDa region, which is processed into 33 and 19 kDa fragments (**Figure 1A**). The 33 kDa fragment contains two high-affinity reticulocyte binding clusters (HARBs) (20 kDa and 14 kDa), and antibodies against the HARBs confer protection in monkeys [10]. In humans, antibodies to the 42 kDa region have also been associated with clinical protection, making this region an attractive vaccine candidate [11–14]. Another vivax protein, PvCSP, is a pre-erythrocytic vaccine candidate and is critical in sporozoite motility and hepatocyte invasion [15]. *P. vivax* circumsporozoite protein has an immunogenic central repeat, consisting of two major types of nonapeptide repeats (VK210 and VK247 – there is also a rarer repeat type termed *vivax-like*) flanked by highly conserved 5' and 3' regions (**Figure 1B**). The *P. falciparum*

Author Summary

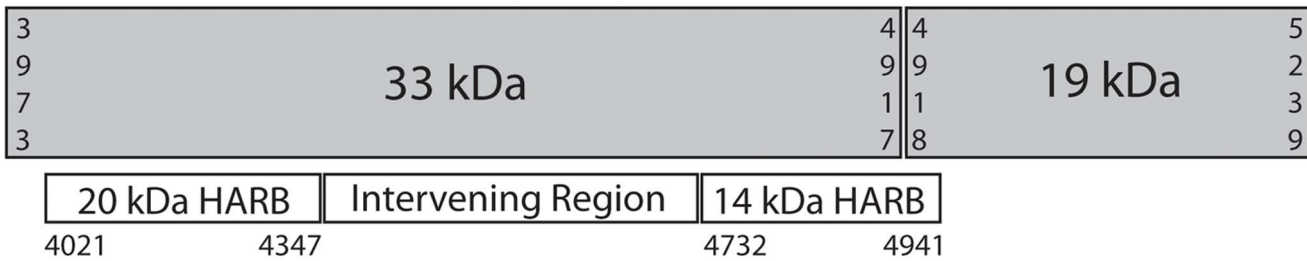
Plasmodium vivax causes tens of millions of malaria cases each year. Although some vaccines against *P. vivax* are being developed, little is known about the geospatial genetic diversity and selective constraints of the parasite surface antigens that these vaccines target. In order to create vaccines that are both efficacious and useful in diverse regions of the world, the strain diversity of these potential vaccine targets must be well understood. Specifically, we must understand whether and how the human immune system develops immunity against these antigens as well as understanding whether these antigens are similar in geographically diverse parasite populations. Here, using next-generation sequencing and population-genetic analyses, we found evidence of likely immune selection in specific regions of two leading vivax vaccine candidate antigens, PvMSP-1 and PvCSP. At the *pvmosp-1* locus, we also found more genetic variability within populations than between populations, with some DNA sequences from geographically diverse populations being highly similar. In contrast, *pvcsp* sequences from geographically diverse populations are very distinct from one another, with specific sequence patterns occurring in certain geographic regions. Our findings provide new insights into the geographic genetic diversity of these two antigens and can help inform the development of effective *P. vivax* vaccines.

Despite this knowledge of PvMSP-1 and PvCSP, little is known about the geospatial genetic diversity of these antigens. Variation in these antigens may become a mechanism of vaccine resistance if strain-specific immunity is important in protection, as has been seen in some *P. falciparum* vaccine candidates [17]. Vaccine trials of *P. falciparum* AMA1 and MSP2 as well as genetic crosses using *P. chabaudi* underscore the importance of strain-specific immunity as a determinant of outcome [18–21]. Additionally, despite initial evidence that strain-specific immunity may not impact RTS,S efficacy [22–25], the incomplete protection afforded by the RTS,S vaccine in Phase II and III trials [16,26,27] has prompted a careful examination of strain-specific responses to this vaccine. Thus, as momentum grows for field trials of *P. vivax* vaccine antigens, carefully designed population genetic studies of *P. vivax* vaccine candidates will be key to assess the need for multivalent vaccine formulations.

To better understand the selective forces on, and geospatial genetic diversity associated with *pvmosp-1* and *pvcsp*, we used the Illumina sequencing platform to determine haplotypes for 42 kDa region of *pvmosp-1* (n = 44) and we used the PacBio and Illumina platforms to sequence the complete *pvcsp* gene (n = 47) from Cambodian isolates [28]. To dissect the immune selection acting on these regions, we studied these sequences using population genetic tests of selection and models of tandem repeat evolution. To evaluate the global genetic diversity of *pvmosp-1* and *pvcsp*, we extracted worldwide *pvmosp-1* and *pvcsp* sequence data available in GenBank (n = 238 for *pvmosp-1* and n = 412 for *pvcsp*) (Figure S1), and studied our sequence data alongside the sequences from GenBank *msp-1*. Finally, we compare the performance of Illumina and PacBio sequencing to traditional Sanger sequencing, and discuss the potential and challenges of next-generation sequencing for population genetic studies of malaria parasite antigens.

ortholog of *pvcsp*, as formulated in RTS,S, is the most advanced *P. falciparum* vaccine candidate to date, showing modest efficacy at one year interim analysis in a Phase III trial [16].

A



B



Figure 1. Protein domains and immunologically-relevant regions of *pvmosp-1* 42 kDa region and *pvcsp*. For both genes, numbers indicate coordinates according to the Sal1 reference genes. Sequences for *pvmosp-1* (PVX_099980) and *pvcsp* (PVX_119355) were accessed August 14, 2012 from PlasmoDB.org. (A) The *pvmosp-1* 42 kDa region is composed of two primary subunits – a 33 kDa and a 19 kDa subunit. Other sub-regions, including the 20 kDa and 14 kDa HARBs have been previously defined and studied. Here, we define the region between the HARBs as the “intervening region.” (B) The *pvcsp* gene is composed of three regions – an N-terminal non-repeat region, a central repeat region, and a C-terminal non-repeat region. The central repeat region consists of two major nonapeptide repeat types, termed VK210 and VK247. Approximate locations of *pvcsp* regions I and II are noted with horizontal lines in the N- and C-terminal non-repeat regions, respectively. doi:10.1371/journal.pntd.0002796.g001

Methods

Parasite isolates

Clinical samples from a previous study were used for this study [29]. Written informed consent was acquired from each individual and the study was approved by the IRB at University of North Carolina, the IRB of the Naval Medical Research Unit #2, Jakarta, Indonesia, and the Cambodian National Ethical Committee for Health Research. Briefly, blood spots were collected from 109 patients with uncomplicated vivax malaria, presenting to a clinic in Chumkiri, Cambodia during 2006–07. We selected 48 subjects with a multiplicity of infection (MOI) of one ($n = 20$) or two ($n = 28$) for sequencing. MOI was determined by heteroduplex tracking assay (HTA) [28,30]. Briefly, in an HTA, radiolabeled DNA probes are annealed to genomic DNA and drawn through a non-denaturing gel matrix. The number of bands observed represents the number of conformation differences present among heteroduplexes, and is a proxy for the number of infection clones (MOI). Details of the method have been published elsewhere [31].

Amplification of *pvmsp-1* and *pvmsp*

The *pvmsp-1* 42 kDa region (nucleotides 3973–5239 of Sall PVX_099980, www.PlasmDB.org) was amplified using primers F: 5'-CAG GAC TAC GCC GAG GAC TA-3' and R: 5'-GGA GGA AAA GCA ACA TGA GC-3' and an Eppendorf Mastercycler (Eppendorf, Hauppauge, NY) in 50 μ L reactions containing 5 μ L 10 \times Qiagen Hotstar Master Mix (Qiagen, Valencia, CA), 0.25 μ L Qiagen Hotstar *Taq*, 300 nM forward primer, 300 nM reverse primer, 1 μ L 10 mM dNTPs, and 5 μ L 5–10 mM template. Cycling conditions were: 95°C \times 15 m; 35 cycles of 95°C \times 45 s, 55°C \times 45 s, 72°C \times 3 m; and 72°C \times 10 m. The *pvmsp* gene (PVX_119355) was performed by nested PCR. The outer step used primers F: 5'-GGC AAA CTC ACA AAC ATC CA-3' and R: 5'-TGC GTA AGC GCA TAA TGT GT-3'. Reactions were as above except for 600 nM forward primer, 600 nM reverse primer, 1 μ L 10 mM dNTPs, 5 μ L 5–10 mM template, 6 μ L of 25 mM MgCl₂, and 28.75 μ L H₂O. Cycling conditions were: 95°C \times 15 m; 25 cycles of 95°C \times 45 s, 45°C \times 45 s, 72°C \times 3 m; and 72°C \times 10 m. The inner step used 600 nM of each of the primers F: 5'-AAA CAG CCA AAG GCC TAC AA-3' and R: 5'-GAC GCC GAA AAT ATT GGA TG-3' using 5–10 μ L of the initial amplification. The cycling conditions were: 95°C \times 15 m; 25 cycles of 95°C \times 45 s, 54°C \times 45 s, 72°C \times 3 m; and 72°C \times 10 m.

Amplicon sequencing and sequence determination

pvmsp-1 and *pvmsp* amplicons were fragmented by acoustic shearing (Covaris, Woburn, MA) using the following settings: 10% duty cycle, 5.0 intensity, 200 cycles per burst, and frequency sweeping mode. Forty-eight barcoded libraries were prepared using the NEXTFlex multiplex library kit (Bioo Scientific, Austin, Texas), each containing the pooled *pvmsp-1* and *pvmsp* amplicons from one patient. Libraries were sequenced on the Illumina HiSeq2000, using the paired-end 100 base pair chemistry (Illumina, San Diego, CA).

We used Lasergene SeqMan NGen v.3.1.1 (DNASTAR, Madison, WI) to assemble *pvmsp-1* short reads *de novo* and to determine SNP frequency within each assembly. For purposes of comparison and confirmation, we re-sequenced 9 *pvmsp-1* amplicons with differing MAFs: 3 samples with all MAFs $>$ 90%; 3 samples with all MAFs between 60% and 90%; 3 samples with MAF $<$ 60% for at least one SNP. Sanger-sequence haplotypes were compared to predicted Illumina haplotypes. Based on these

comparisons, only predicted *pvmsp-1* haplotypes with MAF $>$ 60% at all polymorphic sites were used in our analysis.

In addition to Illumina sequencing, *pvmsp* amplicons were sequenced using PacBio Circular Consensus Sequencing (Pacific Biosciences, Menlo Park, CA). One PacBio SMRT cell produced a total of 12103 reads with a minimum of 3 \times circular consensus coverage, which were used for this study. These were further filtered, removing truncated reads or reads with errors in the barcode. This left 8430 reads (3979 forward and 4451 reverse). Clustering attempted to minimize false positive haplotypes due to erroneous base calls and PCR slippage within the tandem repeat region. For each sample, haplotypes were created by clustering reads, allowing reads differing only by indels of 1 and 2 bases and low quality mismatches to collapse. Low quality was defined as either a mismatching base $Q < 30$ or any $Q < 25$ within an 11 basepair region centered on the mismatch, as has been applied previously to rigorous SNP discovery from shotgun data [32]. To overcome artifacts of PCR infidelity due to slippage events leading to shortened repeats and false haplotypes, we set a high threshold requiring that co-occurring haplotypes of the same repeat type be at high frequency in order to exclude the low frequency variation/stuttering in the repeat region. Haplotype repeat type was then determined by translation and the most frequent haplotype of each major repeat type (VK210 and VK247) present was kept $>$ 0.5%. Additional haplotypes of major repeat types were kept if they were common ($>$ 20%) and thus unlikely to be due simply to low frequency slippage events. In total across all samples 4081 of the 8430 reads clustered contributed to utilized haplotypes.

The long-read haplotypes determined through consensus clustering were used as templates for short-read alignment using Bowtie2 v 2.1.0 [33], with very-sensitive alignment parameters and stringent filtering for Mapping Quality Score and Alignment Score. Final sequence predictions were used for the analyses in this paper and were deposited in GenBank under accession numbers JX461243-JX461285 and KJ173797- KJ173802 for *pvmsp*, and JX461286-JX461333 for *pvmsp-1*.

Rarefaction curves of haplotypes were calculated using EstimateS v9.0. Individual-based curves using sampling without replacement were estimated [34] and extrapolated to 2 \times the actual sample number [35]. Rarefaction plots were visualized in the R base package (<http://cran.us.r-project.org/>).

Acquisition of published sequences for inter-population comparisons

GenBank was queried for population sets published prior to August 1, 2013, which included sequence data for the 42 kDa region of *pvmsp-1* and the whole-gene of *pvmsp*. Sequences from a recent publication [36] were excluded because the isolates were collected over the course of a 12 year period. The authors provide evidence that the haplotype distribution of this population changed substantially over time, making this population inappropriate for our analysis of selection.

Assessing selection on *pvmsp-1* and *pvmsp*

Population datasets with $>$ 25 sequences that were collected over a span of \leq 4 years were included for analysis of selection. We used DnaSP v5.1 to perform tests of selection [37]. We calculated polymorphism and Tajima's D across *pvmsp-1* and the *pvmsp* constant regions using a 50 bp sliding window with a 25 bp step size. We also performed 1000 coalescent simulations with recombination to determine a 95% confidence interval and centile for each Tajima's D estimate [38]. To test for long-term selection, we used the McDonald-Kreitman (MK) test [39]. Skew was calculated using Fisher's exact test (two tailed). For the *pvmsp-1*

42 kDa region amplicons reported here and by others, 15 *Plasmodium knowlesi* *pkmsp-1* isolates from Thailand [40] (Accession Nos. JF837339–JF837353) were used as the interspecies outgroup. Three insertions and deletions occurred in the 42 kDa region of *pvmsp-1* relative to *pkmsp-1*, and were not considered. We could not obtain MK estimates for *pvmsp* sequences due to numerous insertions and deletions relative to *pkmsp*.

For analysis of *pvmsp* repeats, we performed pairwise comparisons of untranslated repeat units within individual *pvmsp* sequences [41]. We calculated skewness and mean nucleotide differences between repeat units, as previously reported [42]. Similar to the methods of Dias et al., 2013, we also calculated dN/dS on the first 1–459 bases of all 32 VK210 repeat regions and the first 1–540 bases of all 15 VK247 repeat regions. This analysis was performed in MEGA5, using the Nei-Gojobori method [43].

Phylogenetics and statistics to determine population structure

Interpopulation heterogeneity was first assessed using Wright's fixation index (F_{ST}). Pairwise fixation values between *pvmsp-1* populations were calculated in DnaSP. Site-specific fixation values for pairwise comparisons among Cambodia, NW Thailand, S Thailand, India, and Turkey were generated using the analysis of molecular variance (AMOVA) function within Arlequin v3.11 [44].

Neighbor-joining trees for *pvmsp-1*, *pvmsp* VK210, and *pvmsp* VK247 were drawn using the APE package for R [45]. To generate trees based off *pvmsp-1*, distance calculations between haplotypes were performed in MEGA5 using the maximum composite likelihood method to construct a neighbor-joining tree file. For the *pvmsp* CR, we used MS_Align (v.2.0) [46,47] to create genetic distance matrices separately comparing both the VK210 and VK247 repeat arrays. MS_Align generates an event-based genetic distance using a model of tandem repeat evolution (expansion, deletion, substitution). Cost parameters for MS_Align were set to 0.1 for amplification or contraction and 5 for repeat insertion or deletion. A pairwise cost table of repeat-to-repeat mutations was created in MEGA5 using the maximum composite likelihood method and used as input for MS_Align [41,48]. MS_Align output matrices were used by FastME [49,50] to construct neighbor-joining trees with balanced branch-length estimation.

To cluster geographic groups, we calculated Hudson's nearest-neighbor statistic (S_{NN}) [51]. Input was in the form of a pairwise distance matrix between all haplotypes for each phylogeny. For this statistic, highly distant populations have values approaching 1 while panmictic populations have values near 0.5. To test the reproducibility of the geographic clustering predicted by S_{NN} , 1000 jackknife samplings were constructed for both *pvmsp-1* and *pvmsp* VK210 and VK247 populations using Fast UniFrac [52]. For each jackknife replicate, 5 individuals, based on the size of the smallest population, were randomly selected from each population and used to redraw trees. Observed splits between geographic populations were quantified and used to assign confidence to predicted geographic clusters. To evaluate potential mutational paths connecting all *pvmsp-1* haplotypes, we constructed a median-joining network using NETWORK v4.6 (Fluxus Engineering, Suffolk, England) [53]. This method expresses multiple plausible evolutionary paths in the form of cycles. A similar analysis was not completed for *pvmsp* due to the variable length of CR haplotypes.

Results

pvmsp-1 sequences

We Illumina sequenced *pvmsp-1* 42 kDa-fragments (Figure 1A) from 48 patients, and compared these to Sanger sequencing data for selected samples. Illumina haplotypes with a major allele frequency of >60% agreed with Sanger haplotypes in every case tested (n = 6). Illumina haplotypes with a major allele frequency of <60% did not consistently agree with Sanger haplotypes (n = 3). Thus, we were able to build 44 complete *pvmsp-1* 42 kDa haplotypes (26 unique haplotypes) with a major allele frequency of >60% at all polymorphic sites (Table 1). The average coverage depth for all isolates was >800 reads per base, with all bases having ≥ 100 reads of coverage. Haplotype accumulation (rarefaction) curves were estimated, and then further extrapolated to show that our sample captured fewer than half the total *pvmsp-1* haplotypes in this region of Cambodia (Figure 2). In addition to these isolates, we identified 238 submissions in GenBank [54–58] (Table S1) containing either the whole-gene or 42 kDa-region sequence information.

Detecting signatures of selection within *pvmsp-1*

The interaction between human host and the parasite has had a profound impact on the parasite genome, leaving behind characteristic “signatures” of natural selection [59], which are detectable using population genetics approaches to examine sequence diversity. We first assessed nucleotide diversity (Figure 3A), and observed a spike of polymorphism in the region between the two HARBs (positions 4348–4731 in the SalI reference). We termed this the “intervening region”. To test whether the diversity in the intervening region is due to long-term selection, we used the McDonald-Kreitman (MK) test [39] to compare the ratio of non-synonymous to synonymous nucleotide polymorphisms between the Cambodian *P. vivax* population and a Thai *P. knowlesi* population [40]. We observed a highly elevated MK ratio ($p = 0.00427$) in the intervening region but not in the HARBs (data not shown) or the entire 42 kDa region ($p = 0.681$), suggesting that the intervening region is under long-term selective pressure (Table 2).

To determine whether the long-term selective pressure shaping the intervening region is potentially due to human immunity, we assessed balancing selection in this region, as balancing selection within a malaria antigen suggests that the antigen is a target of the human immune system [59]. We applied Tajima's D test of neutrality [60] to five geographically distinct *P. vivax* populations (all populations with $n > 25$, accounting for 190 of 238 available sequences) (Table 1, Figure 3B). In panmictic populations with an uncomplicated demographic history [59], the Tajima's D statistic can indicate whether a nucleotide sequence is under directional ($D < 0$) or balancing selection ($D > 0$). Populations not subjected to recent bottlenecks (i.e. Cambodia, India, and NW Thailand, [54,58]) demonstrated a significant signature of balancing selection in the *pvmsp-1* 42 kDa region (Table 1). This signature occurred specifically in the intervening region (Figure 3B), and is consistent with the conclusion that human immunity targets the intervening region.

The three regions of the *pvmsp-1* fragment that are considered vaccine candidates were each assessed for diversity in the Cambodian population [9,61]. In contrast to the intervening region, the 20 kDa HARB (SalI positions 4021–4347) and 14 kDa HARB (SalI positions 4732–4941) showed no coding polymorphisms and no evidence of balancing selection, similar to recent reports [61]. The 19 kDa fragment (SalI nucleotide positions

Table 1. Summary population genetic data for *Plasmodium vivax* antigens.

Country of Origin	n^1	S^2	K^3	π^4	H^5	Hd^6	Tajima's D
<i>pvmsp-1: 42 kDa region</i>							
Cambodia	44	62	24.8	0.020	26	0.950	2.08*
India	28	64	24.9	0.021	27	0.997	1.32*
NW Thailand	65	62	24.9	0.020	34	0.968	2.42*
S Thailand	67	42	6.46	0.005	5	0.336	-0.986
Turkey	30	33	8.33	0.007	3	0.536	-0.001
<i>pvcsp: N- and C-terminal non-repeat regions</i>							
Cambodia	47	-	-	-	24	-	-
N-terminal non-repeat		3	0.971	0.003	3	0.500	0.901
C-terminal non-repeat		2	0.318	0.001	2	0.159	-0.538
Columbia	27	-	-	-	27	-	-
N-terminal non-repeat		2	0.285	0.001	2	0.143	-0.954
C-terminal non-repeat		0	-	-	1	0.000	-

This table includes all population sequence sets which contained sufficient numbers to perform allele-based tests of neutrality. Population sets which included sequence data only for *pvcsp* repeat regions alone are not summarized here.

* $p < 0.05$;

¹number of haplotypes;

²within-population variant sites;

³average number of nucleotide differences;

⁴nucleotide diversity;

⁵number of haplotypes;

⁶haplotype diversity.

doi:10.1371/journal.pntd.0002796.t001

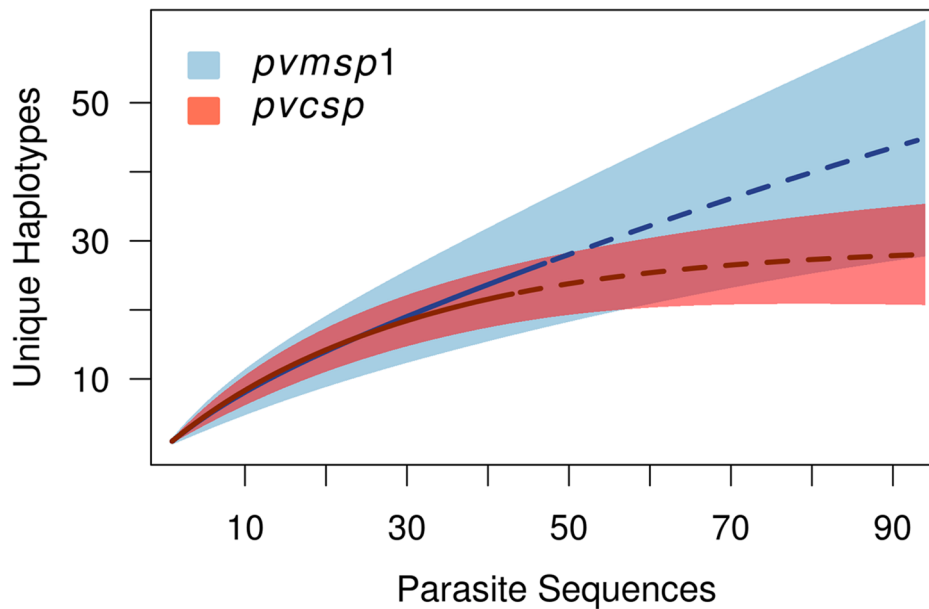


Figure 2. Haplotype rarefaction curves for the Cambodian cohort. Calculated rarefaction curves are depicted by solid blue (*pvmsp-1*) and red (*pvmsp*) lines. Dotted lines represent rarefaction values extrapolated according to the methods of Cowell, et al. The 95% CIs of rarefaction estimates for *pvmsp-1* and *pvmsp* are demarcated by light blue and light red shaded areas, respectively. doi:10.1371/journal.pntd.0002796.g002

4918–5239) also showed limited diversity, with only a K1709E substitution, and no evidence of balancing selection.

Geospatial genetic diversity at the *pvmsp-1* 42 kDa region

Although the *pvmsp-1* 42 kDa region contains potential vaccine candidates [9,61], the 42 kDa region's global genetic diversity has not been carefully evaluated. To study *pvmsp-1* 42 kDa diversity, we calculated Wright's Fixation index (F_{ST}) [62] for each pairwise comparison between five diverse populations (Table 3). F_{ST} values between naturally evolving parasite populations (Cambodia, NW Thailand, and India) approached zero, showing a high degree of genetic similarity, while comparisons with populations that have undergone a recent bottleneck (S Thailand and Turkey) showed a high degree of genetic distance due to their limited number of haplotypes. Similarly, F_{ST} values calculated for each variable site demonstrate a high degree of homogeneity in pairwise comparisons between the Cambodia, NW Thailand, and India populations across all sites, and substantial heterogeneity between S Thailand and Turkey across all sites (Figure S2). This is evidence that balancing selection maintains a similar range of alleles in the *pvmsp-1* 42 kDa region of multiple geographically diverse naturally evolving *P. vivax* populations.

To visualize whether 42 kDa sequences cluster according to geography, we compared all unique haplotypes in a single neighbor-joining tree, which revealed little clustering according to geographic origin (Figure 4). We quantified the extent of this clustering using Hudson's nearest-neighbor statistic (S_{NN}), which assesses how frequently a variant's nearest neighbor is from the same population [51]. In both global and pairwise comparisons, *pvmsp-1* 42 kDa sequences from naturally evolving populations in Cambodia, India, and NW Thailand showed no evidence of strong geographic clustering (Table 4). To further confirm this finding, a neighbor-joining consensus tree was created and underwent 1000 jackknifed replicates (Figure 5A). Results showed that the predicted splits between most populations occurred only

less than 50% of the time, providing strong evidence that there is minimal geographic clustering of *pvmsp-1* 42 kDa sequences.

To better understand the evolutionary relationships between *pvmsp-1* haplotypes from around the world, we employed a median-joining network to describe the set of potential mutational paths between all available global *pvmsp-1* 42 kDa sequences [53]. The network shows extensive admixture of parasite populations from diverse locales, with numerous mutational paths connecting haplotypes (Figure 6). With the exception of populations from S Thailand and Turkey, which have undergone recent bottlenecks, these data provide further evidence that there is no clustering by geography.

pvmsp sequences

We sequenced the complete *pvmsp* gene from 43 isolates using the PacBio and Illumina platforms. *de novo* assembly of the Illumina paired-end short reads was not possible, due to over-collapse in the central repeat (CR) region, resulting in inappropriately short CRs. In contrast, PacBio long reads allowed the gene to be sequenced in its entirety and, after clustering, predicted 47 *pvmsp* haplotypes within the 43 samples. Reported error rates for PacBio sequencing have been high, especially for indels [63]; however, the use of Circular Consensus Sequencing allows single DNA fragments to be read multiple times, decreasing the error rate of the final predicted sequence. To check the accuracy of PacBio *pvmsp* haplotypes, individual haplotypes were used as a template for alignment of Illumina reads from the same clinical isolate. The addition of Illumina reads corrected only a single 1-bp deletion in a single haplotype. Therefore, after clustering, PacBio-predicted haplotypes have an error rate of $1/(\sim 1200 \text{ basepairs/sequence} \times 47 \text{ sequences})$, or approximately 0.002%.

Considering the entire gene, there were 24 unique haplotypes at the nucleotide level, and most genetic diversity was within the CR (Figure 1). Both nonapeptide repeat array types – VK210 (total $n = 32$, range 17–21 repeat units) and VK247 (total $n = 15$, range 20–21 repeat units) – were represented in our Cambodian

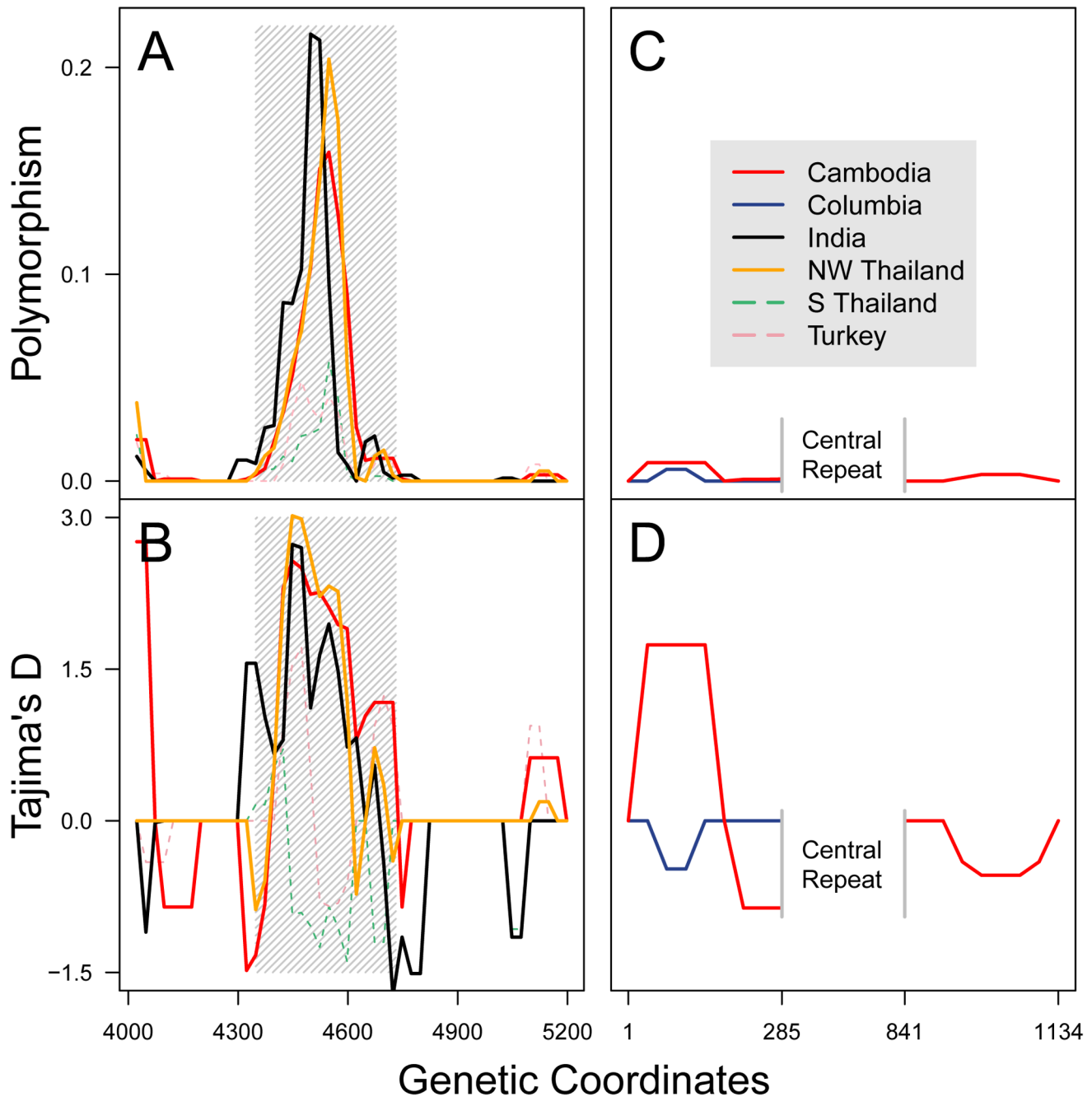


Figure 3. Nucleotide diversity and Tajima's D across the *pvmsp-1* 42 kDa region and the whole *pvmsp* gene. Polymorphism (nucleotide diversity, π) (A) and Tajima's D (B) were calculated across the *pvmsp-1* amplicon for five diverse populations. A sliding window (50 bp window and 25 bp step size) was used to achieve a high resolution analysis. Grey hatches demark the intervening region (nucleotides 4348–4731). For *pvmsp*, N-terminal and C-terminal non-repeat regions were analyzed for nucleotide polymorphism (C) and evidence of balancing selection (D) using a sliding window. Putatively panmictic populations are marked with a solid line, while populations known to be subject to strong selective forces are marked with dotted lines. All coordinates are based on Sal1 *pvmsp-1* and *pvmsp* reference sequences.
doi:10.1371/journal.pntd.0002796.g003

population, with no VK210–VK247 hybrids (reviewed in [64]). The average Illumina short-read depth for each isolate was > 1000, with all bases having ≥ 5 reads of coverage. In addition to our isolates, we identified one cohort of nearly complete *pvmsp* sequences ($n = 27$), and 12 cohorts of CR sequences ($n = 385$) [65–70] (Table 1). An extrapolated rarefaction curve showed that we sampled more than two thirds of the *pvmsp* CR haplotypes in this part of Cambodia, and that there are significantly fewer *pvmsp* CR

variants in this region of Cambodia than *pvmsp-1* 42 kDa variants (Figure 2).

Detecting signatures of selection within *pvmsp*

In contrast to *pvmsp-1*, the 5' and 3' non-repeat regions of *pvmsp* had no significant signatures of selection either by the MK test (data not shown) or Tajima's D test (Table 1). The 5' non-repeat region in the Cambodian cohort showed a non-significant

Table 2. McDonald-Kreitman test for selection in *pvmsp-1*.

McDonald-Kreitman Comparisons				
	42 kDa region		42 kDa intervening region	
	Synonymous	Non-synonymous	Synonymous	Non-synonymous
Fixed	96	93	32	28
Polymorphic	34	39	10	31
	$p = 0.681$		$p = 0.00427$	

Evidence for long-term selective pressure on the *pvmsp-1* 42 kDa region and the 42 kDa intervening region was assessed with the McDonald-Kreitman test, using *P. knowlesi msp1* as the outgroup comparator. A Fisher's exact test (two tailed) was used to determine significance.
doi:10.1371/journal.pntd.0002796.t002

signature of balancing selection (**Table 1 and Figure 3D**), which was due to a G38N amino acid polymorphism. This polymorphism also was observed in 6/16 parasites from the Latin Pacific region (JQ511263-JQ511276, JQ511279, JQ511286) and 2/27 parasites from Colombia (GU339072 and GU339085). The 3' non-repeat region had little evidence of balancing selection, with Tajima's D values ~ 0 (**Table 1 and Figure 3D**). Within *pvmsp*, an 18 amino-acid C-terminal motif known as Region II (amino acid residues 311–328 in Sal1) is important for parasite invasion of hepatocytes [71] and purportedly contains both B and T-cell epitopes [72,73]. Among all Cambodia and Colombia parasite isolates, this motif is completely conserved at the nucleotide and protein level, with an amino-acid sequence of EWTPCS VTCGVGVRVRRR, similar to previous reports [61].

To better understand the selective forces acting upon the *pvmsp* CR, we assessed the dN/dS ratio for Cambodian VK210 and VK247 [66]. Strikingly, synonymous substitutions were strongly favored in both VK210 (dN/dS = 0.267; Z test $p < 0.001$) and VK247 (dN/dS = 0.166; Z test $p < 0.001$) repeats. This is consistent with the finding that VK210 and VK247 isolates from around the world consistently demonstrate a depressed dN/dS ratio, suggesting that the VK210 and VK247 repeat regions are both under strong purifying selection [66].

The CR of *P. falciparum csp* is thought to evolve by slipped-strand mispairing [42]. To understand if a similar mechanism works in the *pvmsp* repeats, we studied the mismatch distribution of pairwise genetic distances between untranslated repeat units within each VK210 and VK247 repeat array type in Cambodia. Consistent with another study [68], we observed a strong right skew in the proportion of genetic differences between pairwise VK210 repeat comparisons, and between pairwise VK247 repeat comparisons,

evidence that *pvmsp* repeats have a high proportion of identical or nearly identical repeats (data not shown). This finding is consistent with a continuous and rapid expansion and contraction of repeats by slipped-strand mispairing, which may be a mechanism to evade host immunity [42].

Geospatial genetic diversity at the *pvmsp* central repeat

A recent study assessed global genetic diversity in the *pvmsp* CR, but did not define the correlates of differentiation between populations [66]. Moreover, this report investigated CR diversity by using a subset of the repeat region that was invariant in length. This approach may not reflect true population structure as it only assesses repeats early in the CR. Indeed, we have found that certain repeat types do cluster in locations within the repeat arrays (data not shown).

To more rigorously study the global diversity of the *pvmsp* CR, we modeled CR repeat expansion, contraction, and substitution using MS_Align, which calculates an event-based genetic distance between CR haplotypes [46]. From these data, we constructed neighbor-joining trees for global VK210 and VK247 repeat arrays isolates (**Figures 7–8**). In contrast to *pvmsp-1*, the VK210 and VK247 trees revealed striking geographic clustering by country and continent. We quantified clustering using Hudson's S_{NN} , and observed strong genetic differentiation between most geographically diverse parasite populations, in contrast to *pvmsp-1* (**Table 4**). To confirm this finding, neighbor-joining consensus trees for both VK210 and VK247 were subjected to 1000 jackknife replicates and the reproducibility of predicted splits between populations was tested demonstrating a strong correlation between genetic distance and geography (**Figure 5B–C**).

Table 3. Interpopulation F_{ST} statistics for *pvmsp-1*.

<i>pvmsp-1</i> Global F_{ST} 0.340				
<i>pvmsp-1</i> Pairwise	Cambodia	India	NW Thailand	S Thailand
India	0.031			
NW Thailand	0.000	0.043		
S. Thailand	0.449	0.433	0.366	
Turkey	0.361	0.329	0.403	0.796

F_{ST} values compare the relatedness of a gene among different populations of the same species. Reported values compare the relatedness of *pvmsp-1* 42 kDa alleles for pairwise comparisons between Cambodia, India, NW Thailand, S Thailand, and Turkey. F_{ST} values approaching 0 indicate greater relatedness, while values approaching 1 indicate substantial inter-population variability. Global F_{ST} statistic calculated between all *pvmsp-1* populations with $n > 25$ indicates that relatively little genetic distance exists between the sampled populations. However, pairwise comparisons demonstrate that some populations exhibit a high degree of genetic similarity (Cambodia and India, for example) while other populations are more dissimilar (S Thailand and Turkey, for example).
doi:10.1371/journal.pntd.0002796.t003

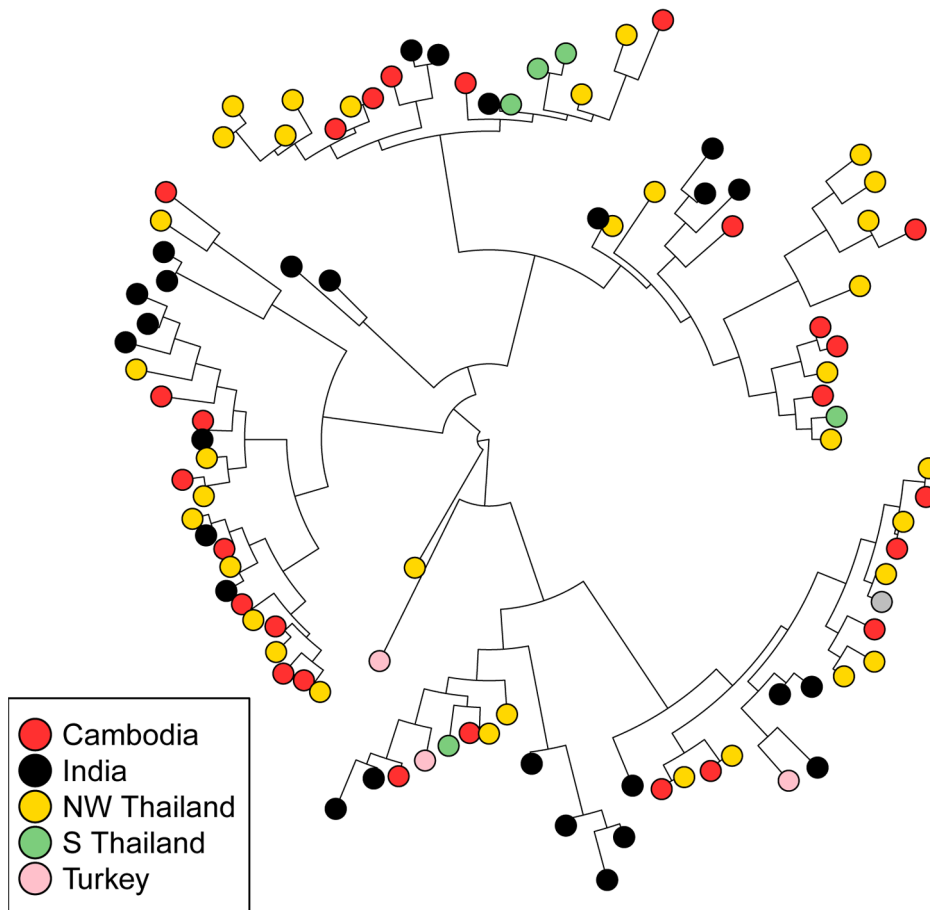


Figure 4. Neighbor-joining tree of 42 kDa regions from *pvmsp-1* isolates. All unique 42 kDa haplotypes from each *pvmsp-1* population set with $n > 25$ were plotted on a single unrooted, neighbor-joining phylogenetic tree. The SalI reference sequence is marked in grey. doi:10.1371/journal.pntd.0002796.g004

We were able to define the peptide sequence basis of the clustering observed among *pvcsp* CR repeats. For VK210 repeats, almost all (81/84) Latin American repeat arrays contained either a 5' (GDRADGQPA)₄ or an internal (GDRADGQPA)₃₋₄, while very few (11/278) of the Asian sequences contained one or both of these features. Similarly, for VK247 repeat arrays, all (34/34) Latin American sequences began with a single EDGAGDQPG repeat, while only one (1/44) Asian sequence began with this repeat. These sequence features may represent a reliable method to assign sequences to a geographic region.

Discussion

This study (1) presents the first population set of *pvmsp-1* and *pvcsp* sequences from Cambodia, (2) identifies a signature of putative immune-mediated, frequency-dependent selection in the *pvmsp-1* 42 kDa region and the *pvcsp* CR, and (3) provides the most comprehensive evaluation to date of geospatial genetic diversity for these genes. We also demonstrate the feasibility of using a next-generation sequencing approach to study the genetic diversity of malaria antigens.

A distinguishing feature of this study is the use of next-generation sequencing methods to generate *P. vivax* amplicon sequence data from clinical isolates. This work represents a first step into this largely unexplored territory. As a relatively new technology, next-generation sequencing methods must be

validated before use in molecular epidemiological studies. We provide evidence that the dominant Illumina-predicted *pvmsp-1* haplotypes are consistent with Sanger sequencing, and are fit for comparison with population sets generated by traditional sequencing methods. Methods for predicting multiple haplotypes from short-read sequencing are under development and will need further validation. We also demonstrate the ability of combined PacBio-Illumina haplotypes to predict *pvcsp* VK210 and VK247 haplotypes out of individual mixed infections. As next-generation sequencing methods are utilized more frequently for population genetic studies of infectious diseases, the methods introduced here will be further improved and will help to provide greater insight into *Plasmodia* population genetics.

Evidence of selection in both *pvmsp-1* and *pvcsp*

We found compelling genetic evidence that the *pvmsp-1* 42 kDa intervening region is under strong immune pressure in multiple panmictic populations. Results from the MK test suggested that this region is under sustained selective pressure (**Table 2**); however, because a positive MK test can signify balancing selection or weak negative selection [74,75], we tested the hypothesis that this region is under balancing selection using Tajima's D test of neutrality. Since multiple populations showed strong evidence of balancing selection by Tajima's D (**Table 1**, **Figure 3B**), we conclude that the intervening region is undergoing continual diversifying, balancing selection. An alter-

Table 4. S_{nm} statistics for the *pvmsp-1* 42 kDa region and the *pvmsp-1* central repeat region.

<i>pvmsp-1</i> Global S_{nm} 0.410*										
	Cambodia	NW Thailand	S Thailand	India						
Cambodia										
NW Thailand	0.318									
S Thailand	0.780	0.865								
India	0.673	0.779*	0.865							
Turkey	0.897	0.946	0.750	0.917						
<i>VK210</i> Global S_{nm} 0.517*										
	Cambodia	Thailand	India	Korea	Tibet	PNG	Sri Lanka	Brazil	Honduras	
Cambodia										
Thailand	0.511									
India	0.824	0.778								
Korea	0.950*	0.92	0.977*							
Tibet	0.968*	1.000*	0.686	0.864						
PNG	0.7621	0.633	0.920*	0.923*	0.913					
Sri Lanka	1.000*	1.000*	0.955*	0.958*	0.926*	0.987*				
Brazil	0.844*	0.958*	0.943*	0.955*	0.969*	0.855	1.000*			
Honduras	0.824	1.000	0.976*	1.000	1.000*	1.000*	1.000*	0.881		
Guatemala	1.000*	0.933	0.970*	1.000	0.957*	0.929	0.960*	0.957*	0.708	
<i>VK247</i> Global S_{nm} 0.872*										
	Cambodia	Thailand	PNG							
Cambodia										
Thailand	1.000*									
PNG	0.904*	0.939*								
Columbia	1.000*	0.981*	0.935*							

S_{nm} values approaching 1 indicate genetic isolation while values near 0.5 indicate that two geographically disparate populations may approximate panmixia. Global and pairwise S_{nm} values show stronger geographic clustering among *pvmsp-1* VK210 and VK247 repeats than among *pvmsp-1* 42 kDa regions.

* indicates significance to ($p \leq 0.05$) after Bonferroni correction for multiple comparisons.

doi:10.1371/journal.pntd.0002796.t004

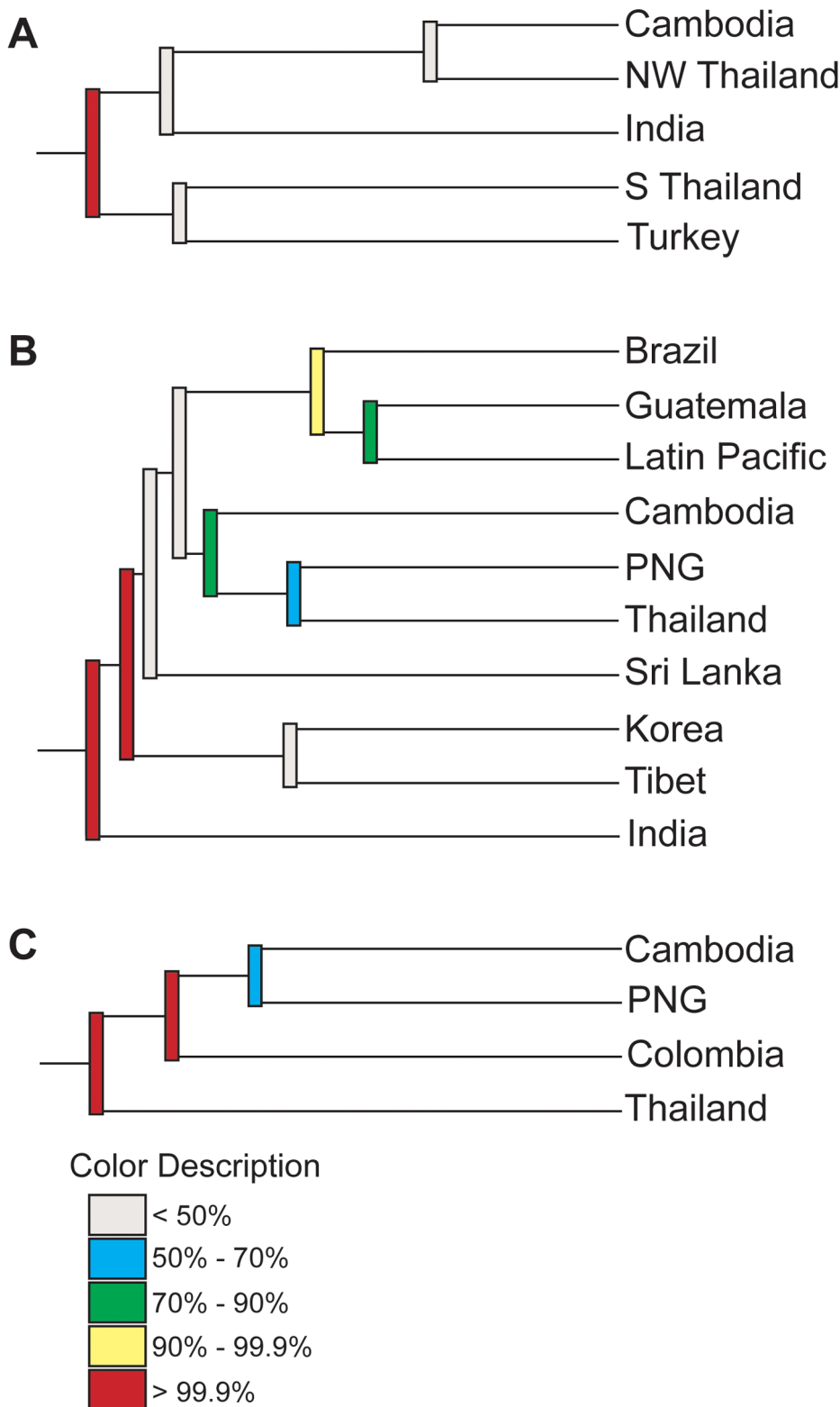


Figure 5. Jackknifed consensus trees demonstrate reproducible geographic clustering in *pvcsp* VK210 and VK247 isolates, but not *pvmsp-1*. The reproducibility of population clustering was assessed using 1000 jackknifed phylogenies. Individual populations clustered together or apart in each of the 1000 jackknifed phylogenies, and the frequency of a split between any two populations was quantified. Populations with grey bars (<50% splits) were genetically similar, while populations with red bars (>99.9% splits) were highly genetically distinct. Phylogenies were built from the *pvmsp-1* 42 kDa region (**A**), the *pvcsp* VK210 central repeat (**B**), and *pvcsp* VK247 central repeat (**C**).
doi:10.1371/journal.pntd.0002796.g005

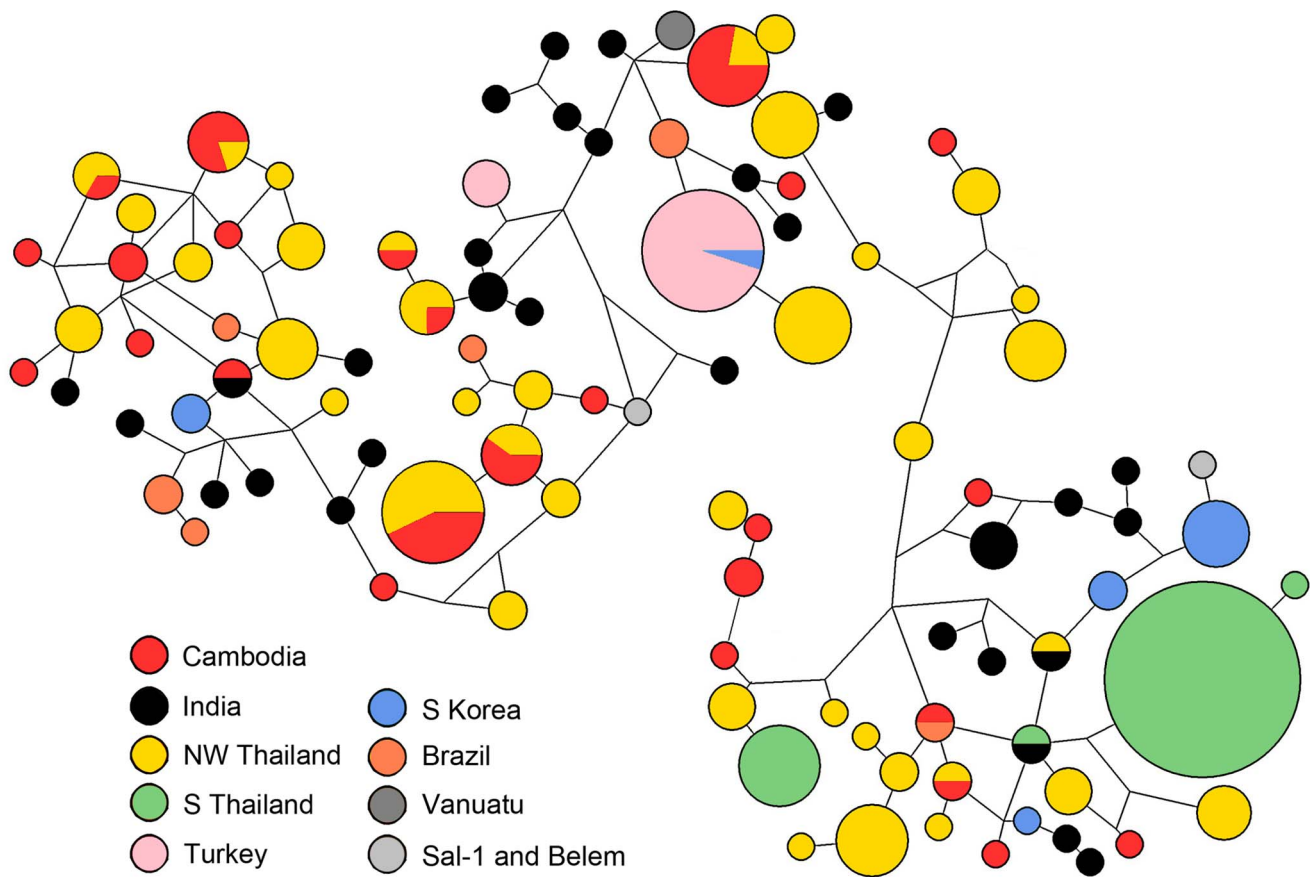


Figure 6. Median-joining network of diverse *pvmsp-1* populations proposes multiple mutational paths between geographically diverse populations. 286 *pvmsp-1* 42 kDa sequences from diverse geographical regions were used as input to create an unrooted median-joining network. This network is a visual representation of the mutational paths that may explain the observed sequence diversity. Each node represents an allele, node size represents the frequency of that allele (range $n=1$ to $n=54$), and node color corresponds to country of origin. Cycles within the diagram represent alternative evolutionary pathways. Corners represent obligate intermediate sequences that were not observed among the sampled alleles. Line length is not proportional to genetic distance.
doi:10.1371/journal.pntd.0002796.g006

native hypothesis is that the positive Tajima's D values are an artifact of recent population contractions. Because (1) a positive Tajima's D was observed in multiple populations, and (2) other regions of *pvmsp-1* contained negative Tajima's D values, we conclude that the 42 kDa intervening region of *pvmsp-1* undergoes frequency-dependent (and likely immune-mediated) balancing selection.

Because PvMSP-1 is a merozoite surface antigen, it is highly accessible to antibodies and complement. The predicted structure of the 42 kDa region shows that the 33 kDa fragment covers the 19 kDa fragment [11,76], limiting its exposure to the human immune system relative to the 33 kDa fragment. This observation could explain the extensive balancing selection present in the 33 kDa fragment (specifically, the intervening region) but not in the 19 kDa fragment. Additionally, this finding suggests that the sliding window approach for evaluating polymorphism and balancing selection may help generate hypotheses about functionally important (19 kDa fragment, for example) or immunologically dominant (the intervening region, for example) regions of *P. vivax* proteins.

For *pvmsp-1*, Tajima's D and F_{ST} were inversely correlated. Populations with strong evidence of high Tajima's D in the *pvmsp-1* intervening region showed a low genetic differentiation by F_{ST} . This suggests that in naturally evolving populations, diversification

of this region is extensive and maintains a similar range of genetic diversity despite geographic distance. Populations that have undergone a recent bottleneck show a low Tajima's D with relatively few variants and strong genetic differentiation from more diverse populations. This suggests that if strain-specific immune responses are important in vaccine efficacy, vaccines may work more effectively if other interventions can be used to bottleneck the population, thus decreasing its genetic diversity [54].

The central repeat region (CR) is a primary immunodominant region of PvCSP. Though alignment-based methods to assess for selection (Tajima's D, for example) cannot be employed in a tandem repeat region, there is wide-ranging evidence that selective pressures shape the genetic composition of the *pvmsp* CR [77–81], including new evidence hinting that hosts develop strain-specific immunity to *P. falciparum* NANP repeats of varying lengths [82]. Indeed, the presence of two distinct repeat types (VK210 and VK247) may itself be evidence of selection as suggested in a study of the *P. cynomolgi csp* CR [80].

Our analysis of the two CR array types, VK210 and VK247, also suggests that selection is occurring in this region. In pairwise comparisons of nucleotide and amino acid differences we observed a positive skew showing decreased differences among repeat units. This finding is consistent with Patil et al.'s study of *pvmsp* isolates from Brazil [68], and provides further evidence that both VK210

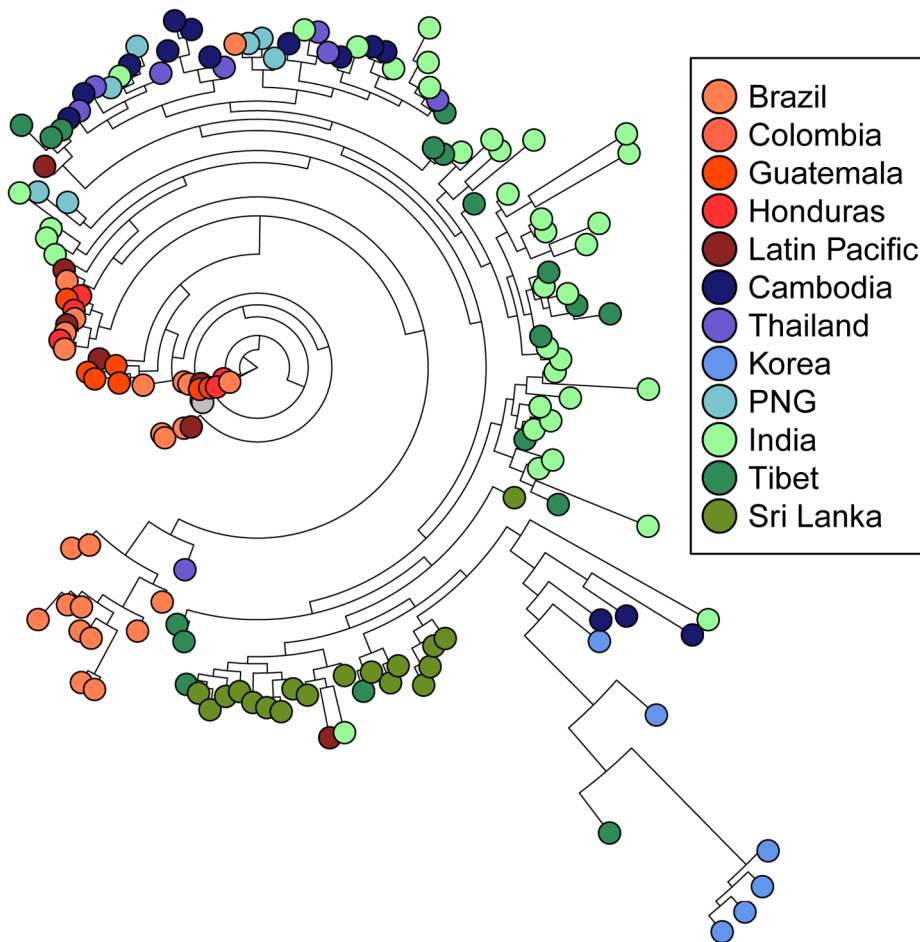


Figure 7. Neighbor-joining tree of *pvmsp* VK210 repeat arrays. All unique repeat array haplotypes from each *pvmsp* VK210 population set were plotted on a single unrooted, neighbor-joining phylogenetic tree. Visual inspection reveals strong geographic clustering by region and country. Latin American sequences are in shades of red, South East Asian sequences are in shades of blue, and South and Central Asian sequences are in shades of green.

doi:10.1371/journal.pntd.0002796.g007

and VK247 repeat arrays may continuously evolve via slipped-strand mispairing [42]. Furthermore, consistent with a recent study of selection in worldwide *pvmsp* isolates [66], we found that Cambodian *pvmsp* VK210 and VK247 isolates have a strong bias toward synonymous substitutions. This signature of purifying selection is consistent with reports from *pfmsp* [83–85] and suggests that there are a limited number of amino acid polymorphisms allowable within this repeat region. Taken together, these findings suggest that expansion, contraction, and rearrangement of repeat units, rather than generation of novel repeat units through mutation, maintain genetic diversity at the *pvmsp* locus in both VK210 and VK247 variants. This phenomenon may be responsible for immune evasion [68,86].

Although these two vivax genes are orthologs of well-characterized vaccine candidate antigens from *P. falciparum* malaria, substantial differences are seen in the effects of immune selection between these genes and their orthologs. Previous reports have shown that the functionally similar *pfmsp-1* 42 kDa fragment has relatively low nucleotide diversity and lacks evidence of balancing selection by Tajima's D [87]. *pfmsp*, on the other hand, shows a high level of nucleotide diversity [88–90] and modest Tajima's D elevations in the C-terminal T cell epitopes [88,91]. These patterns are in stark contrast to our observations in *P. vivax*, and

this highlights the need for *P. vivax*-specific studies to determine appropriate candidate vaccine antigens.

Finally, our analysis of the *pvmsp-1* 42 kDa region underscores the importance of selecting an appropriate parasite population for population-genetic studies. We did not observe signatures of balancing selection in *pvmsp-1* populations from S Thailand or Turkey. This is likely due to bottlenecks secondary to robust malaria control measures employed in S Thailand [54] and limited human migration in Turkey [58]. Thus, appropriate selection of panmictic populations for these studies is critical.

Differing patterns of geospatial genetic diversity at *pvmsp-1* and *pvmsp*

Using both tree-based and statistical methods [92], we found that *pvmsp*, but not *pvmsp-1*, showed strong clustering by geography (Tables 3–4 and Figures 4–8). For *pvmsp-1*, we observed little geographic clustering among naturally evolving parasite populations, suggesting that immune selection maintains similar *pvmsp-1* alleles around the globe. Notably similar findings have been described in Duffy Binding Protein and Thrombospondin-related anonymous protein in vivax malaria [61], while a recent global survey of diversity in the Apical Membrane Antigen 1 found evidence of geographically restricted haplotypes [93]. In contrast

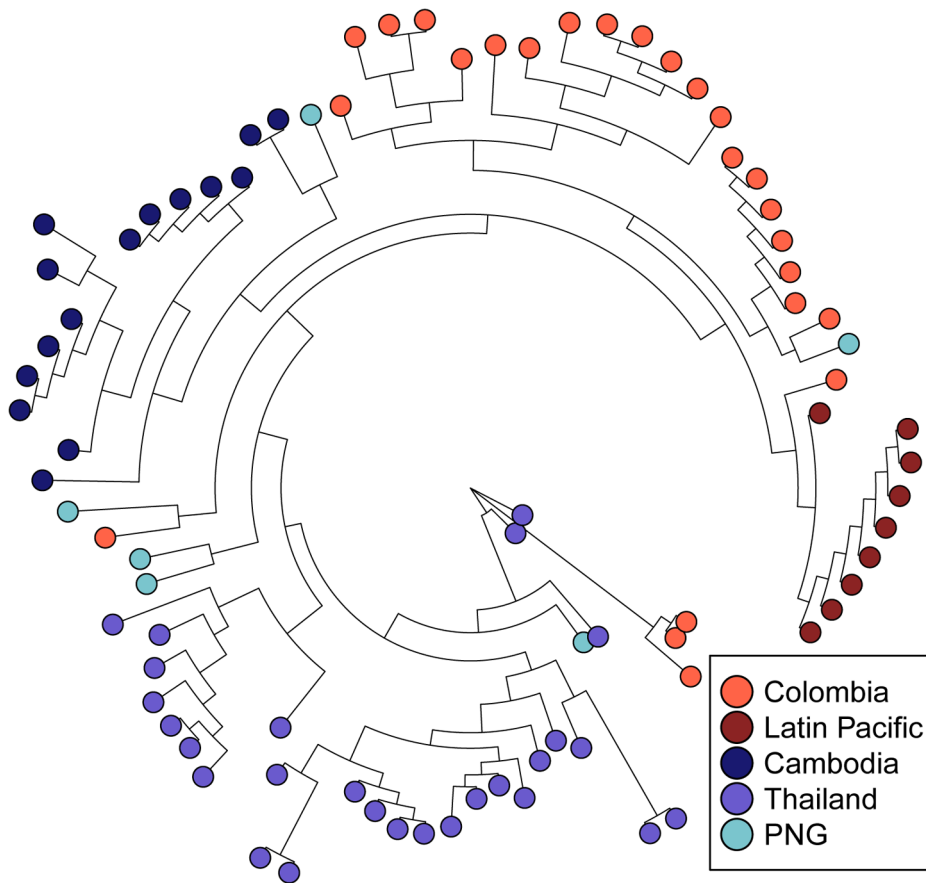


Figure 8. Neighbor-joining tree of *pvcsp* VK247 repeat arrays. All repeat array haplotypes from each *pvcsp* VK247 population set were plotted on a single unrooted, neighbor-joining phylogenetic tree. Latin American sequences are in shades of red, South East Asian sequences are in shades of blue.

doi:10.1371/journal.pntd.0002796.g008

to *pvmssp-1*, we found that *pvcsp* variants demonstrate strong evidence of geographic clustering. This juxtaposition between *pvmssp-1* and *pvcsp* sequences is similar to what has previously been described for merozoite and sporozoite antigens in *P. falciparum* [94]. The population sets included in this survey were collected in different years. While it is known that novel *P. vivax* surface antigen types can appear in the course of a decade [57], it is difficult to assess the magnitude of this effect on our analyses. As more *pvmssp-1* and *pvcsp* population sets are collected, this will become clearer.

It is interesting that the CR of *pvcsp* shows evidence of multiple forms of selection: (1) the depressed number of non-synonymous mutations suggests purifying selection, (2) the differences in CR genotypes between geographic locations suggests directional selection, and (3) the genetic composition of the repeats suggests rapid expansion and contraction, possibly due to immune selection. It is unclear what drives the first two signatures of selection. We hypothesize a model in which purifying selection within a population limits the amino acid composition of repeats due to functional constraints of the protein, while directional selection between populations is driven by environmental factors.

One environmental factor that may explain both the purifying and directional selection of parasite *pvcsp* CR sequences is the mosquito vector. The circumsporozoite protein is expressed in the mosquito during oocyst development [95] and in the salivary glands [96,97]. It is also critical in sporozoite motility [15]. We found no overlap in the distribution of Anopheline species between

the countries from Asia and Latin America included in this study (data not shown) [98–100]. Furthermore, there is substantial evidence that different Anopheline species and strains show differential ability to be infected by malaria [101–104].

Regardless of the cause of the differing patterns of geospatial genetic diversity we observed in *pvmssp-1* and *pvcsp*, the observation itself has significance for vaccine design. The malaria vaccine field is just beginning to unravel how antigenic diversity within a single parasite population can reduce vaccine efficacy [105]. Our findings highlight an additional level of complexity that will hinder the implementation of a vivax vaccine – antigenic variability. While the effects of immune cross-reactivity against different antigenic variants aren't fully known, the extensive intrapopulation variability seen in *pvmssp-1* may necessitate a highly multivalent *pvmssp-1* vaccine, while the dramatic interpopulation variability seen in *pvcsp* suggests that a PvCSP-based vaccine that is effective in one part of the globe may not be effective in other regions. Thus, a thorough understanding of the geospatial genetic diversity of candidate vaccine antigens must inform antigen selection for vaccine design.

GenBank accession numbers

pvcsp sequences: JX461243-JX461285 and KJ173797-KJ173802

pvmssp-1 sequences: JX461286-JX461333

Supporting Information

Figure S1 Geographic distribution of *P. vivax* populations contributing to this study. In total, we identified 13 populations with *pvm**msp-1* 42 kDa fragment sequences and 13 populations with *pvc**sp* central repeat or whole-gene sequences. These populations were collected from 14 countries, pictured above. For countries with $n \geq 10$ isolates, the total number of *pvm**msp-1* and *pvc**sp* isolates is marked. (TIF)

Figure S2 F_{ST} values at polymorphic sites within the *pvmmsp-1* 42 kDa intervening region.** Available parasite populations with $n > 25$ individuals (Cambodia, India, NW Thailand, S Thailand, and Turkey) share 42 variable sites within the 42 kDa intervening region of *pvm**msp-1*. F_{ST} values for each variable site were calculated in a pairwise manner between all five populations. F_{ST} values approaching 0 indicate limited

inter-population variability at that site, while values approaching 1 indicate substantial inter-population variability. Coordinates are reported for every third polymorphic site.

(TIF)

Table S1 *pvmmsp-1* and *pvc**sp* sequences included in this study.** The PlasmoDB gene identifier is PVX_099980 for *pvm**msp-1* and PVX_119355 for *pvc**sp*. *Indicates the year the sequences were made available in GenBank. †Indicates study unpublished but sequences available in GenBank. (DOCX)

Author Contributions

Conceived and designed the experiments: JJJ CMP JAB. Performed the experiments: CMP. Analyzed the data: CMP JJJ JAB NJH. Contributed reagents/materials/analysis tools: DS WOR NJH. Wrote the paper: CMP JJJ JAB.

References

- Mueller I, Galinski MR, Baird JK, Carlton JM, Kochar DK, et al. (2009) Key gaps in the knowledge of Plasmodium vivax, a neglected human malaria parasite. *Lancet Infect Dis* 9: 555–566. doi:10.1016/S1473-3099(09)70177-X.
- Tjitra E, Anstey NM, Sugiarto P, Warikan N, Kenangalem E, et al. (2008) Multidrug-resistant Plasmodium vivax associated with severe and fatal malaria: a prospective study in Papua, Indonesia. *PLoS Med* 5: e128. doi:10.1371/journal.pmed.0050128.
- Price RN, Douglas NM, Anstey NM (2009) New developments in Plasmodium vivax malaria: severe disease and the rise of chloroquine resistance. *Curr Opin Infect Dis* 22: 430–435. doi:10.1097/QCO.0b013e32832f14c1.
- Marfurt J, de Monbrison F, Brega S, Barbolat L, Müller I, et al. (2008) Molecular markers of in vivo Plasmodium vivax resistance to amodiaquine plus sulfadoxine-pyrimethamine: mutations in *pvdhfr* and *pvm**mdr1*. *J Infect Dis* 198: 409–417. doi:10.1086/589882.
- Greenwood B, Targett G (2009) Do we still need a malaria vaccine? *Parasite Immunol* 31: 582–586. doi:10.1111/j.1365-3024.2009.01140.x.
- Baird JK (2013) Evidence and Implications of Mortality Associated with Acute Plasmodium vivax Malaria. *Clin Microbiol Rev* 26: 36–57. doi:10.1128/CMR.00074-12.
- PATH Malaria Vaccine Initiative (2011) Staying the course? Malaria research and development in a time of economic uncertainty.
- Arévalo-Herrera M, Chitnis C, Herrera S (2010) Current status of Plasmodium vivax vaccine. *Hum Vaccin* 6: 124–132.
- Espinosa AM, Sierra AY, Barrero CA, Cepeda LA, Cantor EM, et al. (2003) Expression, polymorphism analysis, reticulocyte binding and serological reactivity of two Plasmodium vivax MSP-1 protein recombinant fragments. *Vaccine* 21: 1033–1043.
- Collins WE, Kaslow DC, Sullivan JS, Morris CL, Galland GG, et al. (1999) Testing the efficacy of a recombinant merozoite surface protein (MSP-1(19)) of Plasmodium vivax in Saimiri boliviensis monkeys. *Am J Trop Med Hyg* 60: 350–356.
- Blackman MJ, Heidrich HG, Donachie S, McBride JS, Holder AA (1990) A single fragment of a malaria merozoite surface protein remains on the parasite during red cell invasion and is the target of invasion-inhibiting antibodies. *J Exp Med* 172: 379–382.
- Guevara Patiño JA, Holder AA, McBride JS, Blackman MJ (1997) Antibodies that inhibit malaria merozoite surface protein-1 processing and erythrocyte invasion are blocked by naturally acquired human antibodies. *J Exp Med* 186: 1689–1699.
- Udhayakumar V, Anyona D, Kariuki S, Shi YP, Bloland PB, et al. (1995) Identification of T and B Cell Epitopes Recognized by Humans in the C-Terminal 42-kDa Domain of the Plasmodium Falciparum Merozoite Surface Protein (MSP)-1. *J Immunol* 154: 6022–6030.
- Nwuba RI, Sodeinde O, Anumudu CI, Omosun YO, Odaibo AB, et al. (2002) The Human Immune Response to Plasmodium falciparum Includes Both Antibodies That Inhibit Merozoite Surface Protein 1 Secondary Processing and Blocking Antibodies. *Infect Immun* 70: 5328–5331. doi:10.1128/IAI.70.9.5328-5331.2002.
- Sultan AA (1999) Molecular mechanisms of malaria sporozoite motility and invasion of host cells. *Int Microbiol Off J Span Soc Microbiol* 2: 155–160.
- Agnandji ST, Lell B, Soulanoudjingar SS, Fernandes JF, Abossolo BP, et al. (2011) First results of phase 3 trial of RTS,S/AS01 malaria vaccine in African children. *N Engl J Med* 365: 1863–1875. doi:10.1056/NEJMoa1102287.
- Takala SL, Plowe CV (2009) Genetic diversity and malaria vaccine design, testing and efficacy: preventing and overcoming “vaccine resistant malaria.” *Parasite Immunol* 31: 560–573. doi:10.1111/j.1365-3024.2009.01138.x.
- Thera MA, Doumbo OK, Coulibaly D, Laurens MB, Ouattara A, et al. (2011) A field trial to assess a blood-stage malaria vaccine. *N Engl J Med* 365: 1004–1013. doi:10.1056/NEJMoa1008115.
- Genton B, Betuela I, Felger I, Al-Yaman F, Anders RF, et al. (2002) A Recombinant Blood-Stage Malaria Vaccine Reduces Plasmodium falciparum Density and Exerts Selective Pressure on Parasite Populations in a Phase 1-2b Trial in Papua New Guinea. *J Infect Dis* 185: 820–827. doi:10.1086/339342.
- Pattaradilokrat S, Cheesman SJ, Carter R (2007) Linkage Group Selection: Towards Identifying Genes Controlling Strain Specific Protective Immunity in Malaria. *PLoS ONE* 2: e857. doi:10.1371/journal.pone.0000857.
- Martinelli A, Cheesman S, Hunt P, Culleton R, Raza A, et al. (2005) A genetic approach to the de novo identification of targets of strain-specific immunity in malaria parasites. *Proc Natl Acad Sci U S A* 102: 814–819. doi:10.1073/pnas.0405097102.
- Enosse S, Dobaño C, Quelhas D, Aponte JJ, Lievens M, et al. (2006) RTS,S/AS02A malaria vaccine does not induce parasite CSP T cell epitope selection and reduces multiplicity of infection. *PLoS Clin Trials* 1: e5. doi:10.1371/journal.pctr.0010005.
- Kumkhaek C, Phra-ek K, Rénia L, Singhasivanon P, Looareesuwan S, et al. (2005) Are Extensive T Cell Epitope Polymorphisms in the Plasmodium falciparum Circumsporozoite Antigen, a Leading Sporozoite Vaccine Candidate, Selected by Immune Pressure? *J Immunol* 175: 3935–3939.
- Allouche A, Milligan P, Conway DJ, Pinder M, Bojang K, et al. (2003) Protective Efficacy of the Rts,s/as02 Plasmodium Falciparum Malaria Vaccine Is Not Strain Specific. *Am J Trop Med Hyg* 68: 97–101.
- Kumkhaek C, Phra-Ek K, Rénia L, Singhasivanon P, Looareesuwan S, et al. (2005) Are extensive T cell epitope polymorphisms in the Plasmodium falciparum circumsporozoite antigen, a leading sporozoite vaccine candidate, selected by immune pressure? *J Immunol Baltim Md* 175: 3935–3939.
- Abdulla S, Salim N, Machera F, Kamata R, Juma O, et al. (2013) Randomized, controlled trial of the long term safety, immunogenicity and efficacy of RTS,S/AS02(D) malaria vaccine in infants living in a malaria-endemic region. *Malar J* 12: 11. doi:10.1186/1475-2875-12-11.
- Olotu A, Fegan G, Wambua J, Nyangweso G, Awuondo KO, et al. (2013) Four-Year Efficacy of RTS,S/AS01E and Its Interaction with Malaria Exposure. *N Engl J Med* 368: 1111–1120. doi:10.1056/NEJMoa1207564.
- Lin JT, Juliano JJ, Kharabora O, Sem R, Lin F-C, et al. (2012) Individual Plasmodium vivax msp1 Variants within Polyclonal P. vivax Infections Display Different Propensities for Relapse. *J Clin Microbiol* 50: 1449–1451. doi:10.1128/JCM.06212-11.
- Rogers WO, Sem R, Tero T, Chim P, Lim P, et al. (2009) Failure of artesunate-mefloquine combination therapy for uncomplicated Plasmodium falciparum malaria in southern Cambodia. *Malar J* 8: 10. doi:10.1186/1475-2875-8-10.
- Givens MB, Lin JT, Lon C, Gosi P, Char MC, et al. (2014) Development of a Capillary Electrophoresis-Based Heteroduplex Tracking Assay To Measure In-Host Genetic Diversity of Initial and Recurrent Plasmodium vivax Infections in Cambodia. *J Clin Microbiol* 52: 298–301. doi:10.1128/JCM.02274-13.
- Ngrenngarmert W, Kwick JJ, Kamwendo DD, Ritola K, Swanstrom R, et al. (2005) Measuring Allelic Heterogeneity in Plasmodium Falciparum by a Heteroduplex Tracking Assay. *Am J Trop Med Hyg* 72: 694–701.
- Altshuler D, Pollara VJ, Cowles CR, Van Etten WJ, Baldwin J, et al. (2000) An SNP map of the human genome generated by reduced representation shotgun sequencing. *Nature* 407: 513–516. doi:10.1038/35035083.
- Langmead B, Salzberg SL (2012) Fast gapped-read alignment with Bowtie 2. *Nat Methods* 9: 357–359. doi:10.1038/nmeth.1923.

34. Colwell RK, Mao CX, Chang J (2004) INTERPOLATING, EXTRA-
POLATING, AND COMPARING INCIDENCE-BASED SPECIES ACCU-
MULATION CURVES. *Ecology* 85: 2717–2727. doi:10.1890/03-0557.
35. Colwell RK, Chao A, Gotelli NJ, Lin S-Y, Mao CX, et al. (2012) Models and
estimators linking individual-based and sample-based rarefaction, extrapolation
and comparison of assemblages. *J Plant Ecol* 5: 3–21. doi:10.1093/jpe/rtr044.
36. Kang J-M, Ju H-L, Kang Y-M, Lee D-H, Moon S-U, et al. (2012) Genetic
polymorphism and natural selection in the C-terminal 42 kDa region of
merozoite surface protein-1 among *Plasmodium vivax* Korean isolates. *Malar J*
11: 206. doi:10.1186/1475-2875-11-206.
37. Librado P, Rozas J (2009) DnaSP v5: a software for comprehensive analysis of
DNA polymorphism data. *Bioinforma Oxf Engl* 25: 1451–1452. doi:10.1093/
bioinformatics/btp187.
38. Hudson RR (1987) Estimating the recombination parameter of a finite
population model without selection. *Genet Res* 50: 245–250.
39. McDonald JH, Kreitman M (1991) Adaptive protein evolution at the *Adh* locus in
Drosophila. *Nature* 351: 652–654. doi:10.1038/351652a0.
40. Jongwutiwes S, Buppan P, Kosuvin R, Seethamchai S, Pattanawong U, et al.
(2011) *Plasmodium knowlesi* Malaria in humans and macaques, Thailand.
Emerg Infect Dis 17: 1799–1806. doi:10.3201/eid1710.110349.
41. Tamura K, Peterson D, Peterson N, Stecher G, Nei M, et al. (2011) MEGA5:
molecular evolutionary genetics analysis using maximum likelihood, evolution-
ary distance, and maximum parsimony methods. *Mol Biol Evol* 28: 2731–2739.
doi:10.1093/molbev/msr121.
42. Hughes AL (2004) The evolution of amino acid repeat arrays in *Plasmodium*
and other organisms. *J Mol Evol* 59: 528–535. doi:10.1007/s00239-004-2645-
4.
43. Nei M, Gojobori T (1986) Simple methods for estimating the numbers of
synonymous and nonsynonymous nucleotide substitutions. *Mol Biol Evol* 3:
418–426.
44. Excoffier L, Laval G, Schneider S (2005) Arlequin (version 3.0): an integrated
software package for population genetics data analysis. *Evol Bioinforma Online*
1: 47–50.
45. Paradis E, Claude J, Strimmer K (2004) APE: Analyses of Phylogenetics and
Evolution in R language. *Bioinformatics* 20: 289–290. doi:10.1093/bioinfor-
matics/btg412.
46. Bérard S, Nicolas F, Buard J, Gascuel O, Rivals E (2006) A fast and specific
alignment method for minisatellite maps. *Evol Bioinforma Online* 2: 303–320.
47. Bérard S, Rivals E (2003) Comparison of minisatellites. *J Comput Biol J Comput
Mol Cell Biol* 10: 357–372. doi:10.1089/10665270360688066.
48. Tamura K, Nei M, Kumar S (2004) Prospects for inferring very large
phylogenies by using the neighbor-joining method. *Proc Natl Acad Sci U S A*
101: 11030–11035. doi:10.1073/pnas.0404206101.
49. Desper R, Gascuel O (2002) Fast and accurate phylogeny reconstruction
algorithms based on the minimum-evolution principle. *J Comput Biol J Comput
Mol Cell Biol* 9: 687–705. doi:10.1089/106652702761034136.
50. Saitou N, Nei M (1987) The neighbor-joining method: a new method for
reconstructing phylogenetic trees. *Mol Biol Evol* 4: 406–425.
51. Hudson RR (2000) A new statistic for detecting genetic differentiation. *Genetics*
155: 2011–2014.
52. Hamady M, Lozupone C, Knight R (2010) Fast UniFrac: facilitating high-
throughput phylogenetic analyses of microbial communities including analysis
of pyrosequencing and PhyloChip data. *ISME J* 4: 17–27. doi:10.1038/
ismej.2009.97.
53. Bandelt HJ, Forster P, Röhl A (1999) Median-joining networks for inferring
intraspecific phylogenies. *Mol Biol Evol* 16: 37–48.
54. Jongwutiwes S, Putaporntip C, Hughes AL (2010) Bottleneck effects on
vaccine-candidate antigen diversity of malaria parasites in Thailand. *Vaccine*
28: 3112–3117. doi:10.1016/j.vaccine.2010.02.062.
55. Putaporntip C, Jongwutiwes S, Sakihama N, Ferreira MU, Kho W-G, et al.
(2002) Mosaic organization and heterogeneity in frequency of allelic
recombination of the *Plasmodium vivax* merozoite surface protein-1 locus.
Proc Natl Acad Sci U S A 99: 16348–16353. doi:10.1073/pnas.252348999.
56. Thakur A, Alam MT, Sharma YD (2008) Genetic diversity in the C-terminal
42 kDa region of merozoite surface protein-1 of *Plasmodium vivax* (PvMSP-
1(42)) among Indian isolates. *Acta Trop* 108: 58–63. doi:10.1016/j.actatrop-
ica.2008.08.011.
57. Han E-T, Wang Y, Lim CS, Cho JH, Chai J-Y (2011) Genetic diversity of the
malaria vaccine candidate merozoite surface protein 1 gene of *Plasmodium*
vivax field isolates in Republic of Korea. *Parasitol Res* 109: 1571–1576.
doi:10.1007/s00436-011-2413-5.
58. Zeyrek FY, Tachibana S-I, Yuksel F, Doni N, Palacpac N, et al. (2010) Limited
polymorphism of the *Plasmodium vivax* merozoite surface protein 1 gene in
isolates from Turkey. *Am J Trop Med Hyg* 83: 1230–1237. doi:10.4269/
ajtmh.2010.10-0353.
59. Weedall GD, Conway DJ (2010) Detecting signatures of balancing selection to
identify targets of anti-parasite immunity. *Trends Parasitol* 26: 363–369.
doi:10.1016/j.pt.2010.04.002.
60. Tajima F (1989) Statistical method for testing the neutral mutation hypothesis
by DNA polymorphism. *Genetics* 123: 585–595.
61. Chenet SM, Tapia LL, Escalante AA, Durand S, Lucas C, et al. (2012) Genetic
diversity and population structure of genes encoding vaccine candidate antigens
of *Plasmodium vivax*. *Malar J* 11: 68. doi:10.1186/1475-2875-11-68.
62. Hudson RR, Slatkin M, Maddison WP (1992) Estimation of levels of gene flow
from DNA sequence data. *Genetics* 132: 583–589.
63. Carneiro MO, Russ C, Ross MG, Gabriel SB, Nusbaum C, et al. (2012) Pacific
biosciences sequencing technology for genotyping and variation discovery in
human data. *BMC Genomics* 13: 375. doi:10.1186/1471-2164-13-375.
64. Lim CS, Tazi L, Ayala FJ (2005) *Plasmodium vivax*: recent world expansion
and genetic identity to *Plasmodium simium*. *Proc Natl Acad Sci U S A* 102:
15523–15528. doi:10.1073/pnas.0507413102.
65. Henry-Halldin CN, Sepe D, Susapu M, McNamara DT, Bockarie M, et al.
(2011) High-throughput molecular diagnosis of circumsporozoite variants
VK210 and VK247 detects complex *Plasmodium vivax* infections in malaria
endemic populations in Papua New Guinea. *Infect Genet Evol J Mol
Epidemiol Evol Genet Infect Dis* 11: 391–398. doi:10.1016/j.mec-
gid.2010.11.010.
66. Dias S, Wickramarachchi T, Sahabandu I, Escalante AA, Udagama PV (2013)
Population genetic structure of the *Plasmodium vivax* circumsporozoite protein
(Pvcsp) in Sri Lanka. *Gene* 518: 381–387. doi:10.1016/j.gene.2013.01.003.
67. Hernández-Martínez MA, Escalante AA, Arévalo-Herrera M, Herrera S
(2011) Antigenic diversity of the *Plasmodium vivax* circumsporozoite protein in
parasite isolates of Western Colombia. *Am J Trop Med Hyg* 84: 51–57.
doi:10.4269/ajtmh.2011.09-0785.
68. Patil A, Orjuela-Sánchez P, da Silva-Nunes M, Ferreira MU (2010)
Evolutionary dynamics of the immunodominant repeats of the *Plasmodium*
vivax malaria-vaccine candidate circumsporozoite protein (CSP). *Infect Genet
Evol J Mol Epidemiol Evol Genet Infect Dis* 10: 298–303. doi:10.1016/
j.mecgid.2010.01.006.
69. Santos-Ciminera PD, Alecrim M das GC, Roberts DR, Quinlan GV Jr (2007)
Molecular epidemiology of *Plasmodium vivax* in the State of Amazonas, Brazil.
Acta Trop 102: 38–46. doi:10.1016/j.actatropica.2007.02.013.
70. Lopez AC, Ortiz A, Coello J, Sosa-Achoa W, Torres REM, et al. (2012)
Genetic diversity of *Plasmodium vivax* and *Plasmodium falciparum* in
Honduras. *Malar J* 11: 391. doi:10.1186/1475-2875-11-391.
71. Cerami C, Kwakye-Berko F, Nussenzweig V (1992) Binding of malarial
circumsporozoite protein to sulfatides [Gal(3-SO₄)beta 1-Cer] and cholesterol-
3-sulfate and its dependence on disulfide bond formation between cysteines in
region II. *Mol Biochem Parasitol* 54: 1–12.
72. Sinnis P, Clavijo P, Fenyo D, Chait BT, Cerami C, et al. (1994) Structural and
functional properties of region II-plus of the malaria circumsporozoite protein.
J Exp Med 180: 297–306.
73. Seth RK, Bhat AA, Rao DN, Biswas S (2010) Acquired immune response to
defined *Plasmodium vivax* antigens in individuals residing in northern India.
Microbes Infect 12: 199–206. doi:10.1016/j.micinf.2009.12.006.
74. Teteh KKA, Stewart LB, Ochola LI, Amambua-Ngwa A, Thomas AW, et al.
(2009) Prospective Identification of Malaria Parasite Genes under Balancing
Selection. *PLoS ONE* 4: e5568. doi:10.1371/journal.pone.0005568.
75. Charlesworth J, Eyre-Walker A (2008) The McDonald–Kreitman Test and
Slightly Deleterious Mutations. *Mol Biol Evol* 25: 1007–1015. doi:10.1093/
molbev/msn005.
76. Blackman MJ, Whittle H, Holder AA (1991) Processing of the *Plasmodium*
falciparum major merozoite surface protein-1: identification of a 33-kilodalton
secondary processing product which is shed prior to erythrocyte invasion. *Mol
Biochem Parasitol* 49: 35–44. doi:10.1016/0166-6851(91)90128-S.
77. Arnot DE, Barnwell JW, Tam JP, Nussenzweig V, Nussenzweig RS, et al.
(1985) Circumsporozoite protein of *Plasmodium vivax*: gene cloning and
characterization of the immunodominant epitope. *Science* 230: 815–818.
doi:10.1126/science.2414847.
78. Arevalo-Herrera M, Roggero MA, Gonzalez JM, Vergara J, Corradin G, et al.
(1998) Mapping and comparison of the B cell epitopes recognized on the
Plasmodium vivax circumsporozoite protein by immune Colombians and
immunized Aotus monkeys. *Ann Trop Med Parasitol* 92: 539–551.
doi:10.1080/00034989859230.
79. Herrera S, Escobar P, Plata C de, Avila GI, Corradin G, et al. (1992) Human
recognition of T cell epitopes on the *Plasmodium vivax* circumsporozoite
protein. *J Immunol* 148: 3986–3990.
80. Hughes AL (1991) Circumsporozoite protein genes of malaria parasites
(*Plasmodium* spp.): evidence for positive selection on immunogenic regions.
Genetics 127: 345–353.
81. Nardin E, Clavijo P, Mons B, Belkum A van, Ponnudurai T, et al. (1991) T cell
epitopes of the circumsporozoite protein of *Plasmodium vivax*. Recognition by
lymphocytes of a sporozoite-immunized chimpanzee. *J Immunol* 146: 1674–
1678.
82. Bowman NM, Congdon S, Mvalo T, Patel JC, Escamilla V, et al. (2013)
Comparative population structure of *Plasmodium falciparum* circumsporozoite
protein NANP repeat lengths in Lilongwe, Malawi. *Sci Rep* 3: 1990.
doi:10.1038/srep01990.
83. Escalante AA, Lal AA, Ayala FJ (1998) Genetic polymorphism and natural
selection in the malaria parasite *Plasmodium falciparum*. *Genetics* 149: 189–
202.
84. Rich SM, Hudson RR, Ayala FJ (1997) *Plasmodium falciparum* antigenic
diversity: Evidence of clonal population structure. *Proc Natl Acad Sci U S A*
94: 13040–13045.
85. Hartl DL (2004) The origin of malaria: mixed messages from genetic diversity.
Nat Rev Microbiol 2: 15–22. doi:10.1038/nrmicro795.

86. Ferreira MU, Hartl DL (2007) *Plasmodium falciparum*: Worldwide sequence diversity and evolution of the malaria vaccine candidate merozoite surface protein-2 (MSP-2). *Exp Parasitol* 115: 32–40. doi:10.1016/j.exppara.2006.05.003.
87. Pacheco MA, Poe AC, Collins WE, Lal AA, Tanabe K, et al. (2007) A comparative study of the genetic diversity of the 42 kDa fragment of the merozoite surface protein 1 in *Plasmodium falciparum* and *P. vivax*. *Infect Genet Evol* 7: 180–187. doi:10.1016/j.meegid.2006.08.002.
88. Bailey JA, Mvalo T, Aragam N, Weiser M, Congdon S, et al. (2012) Use of Massively Parallel Pyrosequencing to Evaluate the Diversity of and Selection on *Plasmodium falciparum* csp T-Cell Epitopes in Lilongwe, Malawi. *J Infect Dis* 206: 580–587. doi:10.1093/infdis/jis329.
89. Jalloh A, Jalloh M, Matsuoka H (2009) T-cell epitope polymorphisms of the *Plasmodium falciparum* circumsporozoite protein among field isolates from Sierra Leone: age-dependent haplotype distribution? *Malar J* 8: 120. doi:10.1186/1475-2875-8-120.
90. Gandhi K, Thera MA, Coulibaly D, Traoré K, Guindo AB, et al. (2012) Next generation sequencing to detect variation in the *Plasmodium falciparum* circumsporozoite protein. *Am J Trop Med Hyg* 86: 775–781. doi:10.4269/ajtmh.2012.11-0478.
91. Weedall GD, Preston BMJ, Thomas AW, Sutherland CJ, Conway DJ (2007) Differential evidence of natural selection on two leading sporozoite stage malaria vaccine candidate antigens. *Int J Parasitol* 37: 77–85. doi:10.1016/j.ijpara.2006.09.001.
92. Zárate S, Pond SLK, Shapshak P, Frost SDW (2007) Comparative Study of Methods for Detecting Sequence Compartmentalization in Human Immunodeficiency Virus Type 1. *J Virol* 81: 6643–6651. doi:10.1128/JVI.02268-06.
93. Arnott A, Mueller I, Ramsland PA, Siba PM, Reeder JC, et al. (2013) Global Population Structure of the Genes Encoding the Malaria Vaccine Candidate, *Plasmodium vivax* Apical Membrane Antigen 1 (PvAMA1). *PLoS Negl Trop Dis* 7: e2506. doi:10.1371/journal.pntd.0002506.
94. Barry AE, Schultz L, Buckee CO, Reeder JC (2009) Contrasting population structures of the genes encoding ten leading vaccine-candidate antigens of the human malaria parasite, *Plasmodium falciparum*. *PLoS One* 4: e8497. doi:10.1371/journal.pone.0008497.
95. Boulanger N, Charoenvit Y, Krettli A, Betschart B (1995) Developmental changes in the circumsporozoite proteins of *Plasmodium berghei* and *P. gallinaceum* in their mosquito vectors. *Parasitol Res* 81: 58–65.
96. Posthuma G, Meis JF, Verhave JP, Hollingdale MR, Ponnudurai T, et al. (1988) Immunogold localization of circumsporozoite protein of the malaria parasite *Plasmodium falciparum* during sporogony in *Anopheles stephensi* midguts. *Eur J Cell Biol* 46: 18–24.
97. Golenda CF, Starkweather WH, Wirtz RA (1990) The distribution of circumsporozoite protein (CS) in *Anopheles stephensi* mosquitoes infected with *Plasmodium falciparum* malaria. *J Histochem Cytochem Off J Histochem Soc* 38: 475–481.
98. WHO World Malaria Report (2011). Available: <http://www.who.int/malaria/publications/atoz/9789241564403/en/index.html>.
99. Foley DH, Klein TA, Lee I-Y, Kim M-S, Wilkerson RC, et al. (2011) Mosquito species composition and *Plasmodium vivax* infection rates on Baengnyeong-do (island), Republic of Korea. *Korean J Parasitol* 49: 313–316. doi:10.3347/kjp.2011.49.3.313.
100. Yoo D-H, Shin E-H, Park M-Y, Kim HC, Lee D-K, et al. (2013) Mosquito species composition and *Plasmodium vivax* infection rates for Korean army bases near the demilitarized zone in the Republic of Korea, 2011. *Am J Trop Med Hyg* 88: 24–28. doi:10.4269/ajtmh.2012.11-0755.
101. Adak T, Singh OP, Das MK, Wattal S, Nanda N (2005) Comparative susceptibility of three important malaria vectors *Anopheles stephensi*, *Anopheles fluviatilis*, and *Anopheles sondaicus* to *Plasmodium vivax*. *J Parasitol* 91: 79–82. doi:10.1645/GE-3514.
102. Marrelli MT, Honório NA, Flores-Mendoza C, Lourenço-de-Oliveira R, Marinotti O, et al. (1999) Comparative susceptibility of two members of the *Anopheles oswaldoi* complex, *An. oswaldoi* and *An. konderi*, to infection by *Plasmodium vivax*. *Trans R Soc Trop Med Hyg* 93: 381–384.
103. Joshi D, Chochoate W, Park M-H, Kim J-Y, Kim T-S, et al. (2009) The susceptibility of *Anopheles lesteri* to infection with Korean strain of *Plasmodium vivax*. *Malar J* 8: 42. doi:10.1186/1475-2875-8-42.
104. Da Silva ANM, Santos CCB, Lacerda RN, Machado RLD, Póvoa MM (2006) Susceptibility of *Anopheles aquasalis* and *an. darlingi* to *Plasmodium vivax* VK210 and VK247. *Mem Inst Oswaldo Cruz* 101: 547–550.
105. Takala SL, Coulibaly D, Thera MA, Batchelor AH, Cummings MP, et al. (2009) Extreme Polymorphism in a Vaccine Antigen and Risk of Clinical Malaria: Implications for Vaccine Development. *Sci Transl Med* 1: 2ra5. doi:10.1126/scitranslmed.3000257.